Available online at www.sciencedirect.com
SCIENCE DIRECT®
Journal of Power Sources 144 (2005) 255–261
JOURNAL OF POWER SOURCES
www.elsevier.com/locate/jpowsour

Microstructures and electrochemical performances of $La_2Mg(Ni_{0.85}Co_{0.15})_9Cr_x$ ($x = 0$–0.2) electrode alloys prepared by casting and rapid quenching

Yang-Huan Zhang[a,b,*], Xiao-Ping Dong[a], Guo-Qing Wang[a], Shi-Hai Guo[b], Xin-Lin Wang[b]

[a] *School of Material, Inner Mongolia University of Science and Technology, Baotou 014010, China*
[b] *Department of Functional Material Research, Central Iron and Steel Research Institute, 76 Xuanyuannan Road, Haidian District, Beijing 100081, China*

Received 9 August 2004; received in revised form 16 November 2004; accepted 16 November 2004
Available online 12 January 2005

Abstract

In order to improve the electrochemical cycle stability of La–Mg–Ni system ($PuNi_3$-type) hydrogen storage alloy, a trace of Cr was added and rapid quenching techniques were employed. The electrochemical performances and microstructures of the as-cast and -quenched alloys were determined and measured. The effects of Cr content and quenching rate on the microstructures and electrochemical properties of the alloys were investigated in detail. The obtained results show that the as-cast and -quenched alloys are composed of the (La, Mg)Ni_3 phase ($PuNi_3$-type structure) and the $LaNi_5$ phase as well as the $LaNi_2$ phase. The amount of the $LaNi_2$ phase increases with the increase of Cr content. The addition of Cr enhances the cycle stability of the as-cast and -quenched alloys, but decreases the discharge capacities of the alloys. The cycle lives of the alloys increase with the increase of the quenching rate. The as-cast and -quenched alloys have an excellent activation performance.

Keywords: La–Mg–Ni system electrode alloy; Rapid quenching technique; Microstructure; Electrochemical performance

1. Introduction

Ni-MH batteries have been used widely by virtue of several of their advantages, such as high capacity, capable of performing a high rate charge–discharge, high resistance to overcharging and over-discharging, a long cycle life, environmental friendliness, and interchangeability with Ni–Cd batteries [1]. A series of metal hydride electrode alloys have been discovered, including the rare-earth-based AB_5-type alloys [2], the AB_2-type Laves phase alloys [3], the V-based solid solution alloys [4], and the Mg-based alloys [5,6]. Among the hydrogen storage alloys mentioned above, the discharge capacity of the AB_5-type electrode alloys is comparatively low, the activation of the AB_2-type Laves phase electrode alloys is very difficult, the electrocatalytic activation of the V-based solid solution alloys is also difficult, and the cycle stability of the Mg-based electrode alloys is extremely poor. In the very recent years, however, the rechargeable Ni-MH cells are encountering serious competition owing to rapid development of Li-ion cells [7]. Therefore, investigations of new type electrode alloys with higher capacity and longer cycle life are very important to exalt the competition ability of Ni-MH batteries in the rechargeable battery field. Several new and good hydrogen storage alloys were reported recently. One of the most promising candidates is the La–Mg–Ni system for increasing the capacity. Oesterreicher and Bittner [8] have reported that $La_{1-x}Mg_xNi_2$ ($x = 0$–1.0) alloys are superior to $LaNi_5$-type alloys or Laves phase AB_2-type alloys as to the hydrogen absorption capacity. After investigating the electrochemical performances of the La_2MgNi_9, $La_5Mg_2Ni_{23}$ and

* Corresponding author. Tel.: +86 10 62187570; fax: +86 10 62182296.
E-mail addresses: ljlgrace@vip.sina.com, zyh59@yahoo.com.cn (Y.-H. Zhang).

0378-7753/$ – see front matter © 2004 Elsevier B.V. All rights reserved.
doi:10.1016/j.jpowsour.2004.11.043

La_3MgNi_{14}-type electrode alloys, Kohno et al. [6] found that the $La_5Mg_2Ni_{23}$-type electrode alloy $La_{0.7}Mg_{0.3}Ni_{2.8}Co_{0.5}$ has a capacity of 410 mAh g^{-1} and good cycle stability during 30 charge–discharge cycles. The hydrogen storage alloy system with the general formula of R_2MgNi_9 (R = rare earth or Ca element) is a very promising system for the reversible absorption/desorption of gaseous hydrogen. Kadir et al. [9] investigated the structure of the R_2MgNi_9 (R = La, Ce, Pr, Nd, Sm and Gd) alloys and the result obtained shows that the alloys have the $PuNi_3$-type structure. Pan et al. [10] have investigated the structures and electrochemical characteristics of the $La_{0.7}Mg_{0.3}(Ni_{0.85}Co_{0.15})_x$ (x = 3.15–3.80) alloy system and obtained a maximum discharge capacity of 398 mAh g^{-1}, but the cycle stability of the alloy needs to be improved further. In order to improve further the cycle stability of the $PuNi_3$-type $La_2Mg(Ni_{0.85}Co_{0.15})_9$ electrode alloy, a trace of Cr was added and rapid quenching techniques were employed. The obtained results show that the cycle stabilities of the experimental alloys could be improved significantly.

2. Experimental

2.1. Preparation of alloys

The alloys were melted in an argon atmosphere using a vacuum induction furnace. In order to prevent the volatilization of element Mg during melting, a positive argon pressure of 0.1 MPa was applied. After induction melting, the melt was poured into a copper mould cooled by water, and a cast ingot was obtained. Part of the as-cast alloys was re-melted and quenched by melt-spinning with a rotating copper wheel. Flakes of the as-quenched alloys were obtained with quenching rates of 15, 20, 25 and 30 m s^{-1}. The quenching rate is expressed by the linear velocity of the copper wheel. The chemical compositions of the alloys are $La_2Mg(Ni_{0.85}Co_{0.15})_9Cr_x$ (x = 0, 0.1 and 0.2). The alloys are represented by Cr_0, Cr_1 and Cr_2, respectively. The purity of all the component metals La, Ni, Co, Mg, Cr is at lest 99.7 wt.%.

2.2. Microstructure determination

The samples of the as-cast alloys were directly polished. The samples thus prepared were etched with a 60% HF solution. The morphologies of the as-cast and -quenched alloys were examined by SEM. The samples of the as-cast and -quenched alloys were pulverized by mechanical grinding, and the sizes of the powder sample particles were less than 75 μm. The phase structures of the alloys were determined by XRD. The type of X-ray diffractometer used in this experiment is D/max/2400. The diffraction was performed with Cu $K\alpha_1$ radiation and the rays were filtered by graphite. The experimental parameters for determining phase structure are 160 mA, 40 kV and 10° min^{-1}, respectively. The powder samples were dispersed in anhydrous alcohol for observing the grain morphology with TEM, and for determining crystalline state of the samples with selected area electron diffraction (SAD).

2.3. Electrode preparation and electrochemical measurement

The fractions of the as-cast and -quenched alloys, which were ground mechanically into powder below 250 mesh, were used for the preparation of the experimental electrode. Electrode pellets with 15 mm diameter were prepared by mixing 1 g alloy powder and 1 g Ni powder as well as a small amount of polyvinyl alcohol (PVA), and then compressing under a pressure of 35 MPa. After drying for 4 h, the electrode pellets were immersed in 6 M KOH solution for 24 h in order to wet fully the electrodes before the electrochemical measurement.

The electrode pellet was fixed on the outgoing line of a negative electrode of an open tri-electrode cell and the electrochemical characteristics were measured. $Ni(OH)_2$/NiOOH is the positive electrode of the experimental cell, Hg/HgO the reference electrode and 6 M KOH solution the electrolyte. The voltage between the negative electrode and the reference electrode is defined as the discharge voltage. In every cycle, the negative electrode was charged with constant current of 100 mA g^{-1} for 5 h, rested for 15 min and then discharged at 100 mA g^{-1} to −0.500 V cut-off voltage. The environment temperature of measurement was kept at 30 °C.

3. Results and discussion

3.1. Electrochemical performances of the alloys

3.1.1. Activation performance

The activation performance is characterized by the initial activation number. The initial activation number denoted by n is defined as the number of charge–discharge cycles required for attaining the maximum discharge capacity through a charge–discharge cycle at a constant current density of 100 mA g^{-1}. The cycle number dependence of the discharge capacity of the as-cast and -quenched alloys is illustrated in Fig. 1, the charge–discharge current density being 100 mA g^{-1}. It can be derived from Fig. 1 that all of the as-cast and -quenched alloys have an excellent activation performance, and the as-cast and -quenched alloys can be completely activated after 2–3 cycles. The results show that the addition of Cr can improve the activation performances of the as-cast alloys.

3.1.2. Discharge capacity

The maximum discharge capacities of the as-cast and -quenched alloys were measured with a constant current density of 100 mA g^{-1}. The quenching rate dependence of the maximum discharge capacity of the alloy is shown in Fig. 2. It can be derived from Fig. 2 that the discharge capacities of the

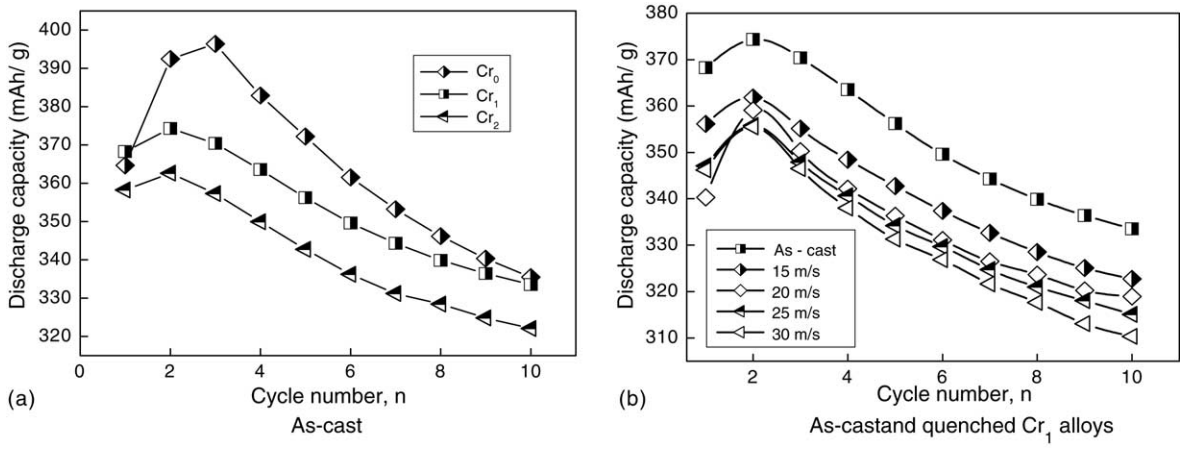

Fig. 1. The cycle number dependence of the discharge capacity of the alloys: (a) as-cast; (b) as-cast and -quenched Cr_1 alloys.

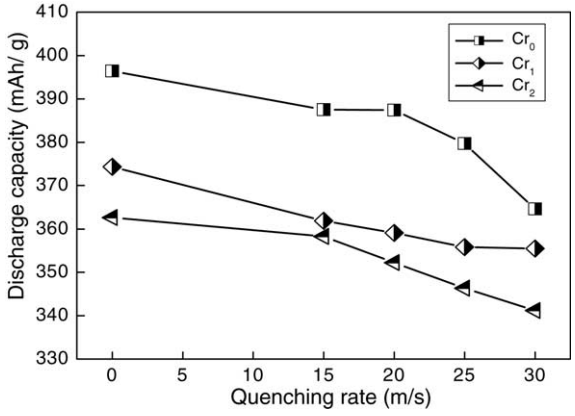

Fig. 2. The relationship between the quenching rate and the maximum discharge capacity.

as-cast and -quenched alloys decrease with the increase of Cr content. When Cr content increased from 0 to 0.2, the maximum capacities of the as-cast alloys were decreased from 396 to 364 mAh g^{-1}. For the as-quenched alloys obtained with a quenching rate of 15 ms, the maximum capacities were decreased from 387 to 358 mAh g^{-1}. In addition, the capacities of the alloys were decreased after rapid quenching. When the quenching rate increased from 0 m s^{-1} (as-cast was defined as quenching rate of 0 m s^{-1}) to 30 m s^{-1}, the maximum capacities of the Cr_1 alloys were decreased from 374 to 355 mAh g^{-1}.

3.1.3. Cycle life

The cycle life, indicated by *N*, is characterized by the cycle number after which the discharge capacity of the alloy obtained with a current density of 100 mA g^{-1} is reduced to 60% of the maximum capacity. The cycle number dependence of the discharge capacities of the as-cast and -quenched alloys is shown in Fig. 3. The results given in Fig. 3(a) show that the slopes of the curves decrease with the increase of Cr content. Fig. 3(b) shows that the slopes of the curves decrease with the increase of the quenching rate. The results indicate that addition Cr and rapid quenching treatment are favourable for the cycle stabilities of the alloys. In order to show the effect of the quenching rate on the cycle life of the alloy, the quenching rate dependence of the cycle lives of the alloys is illustrated in Fig. 4. Fig. 4 shows that the cycle lives of the as-cast alloys

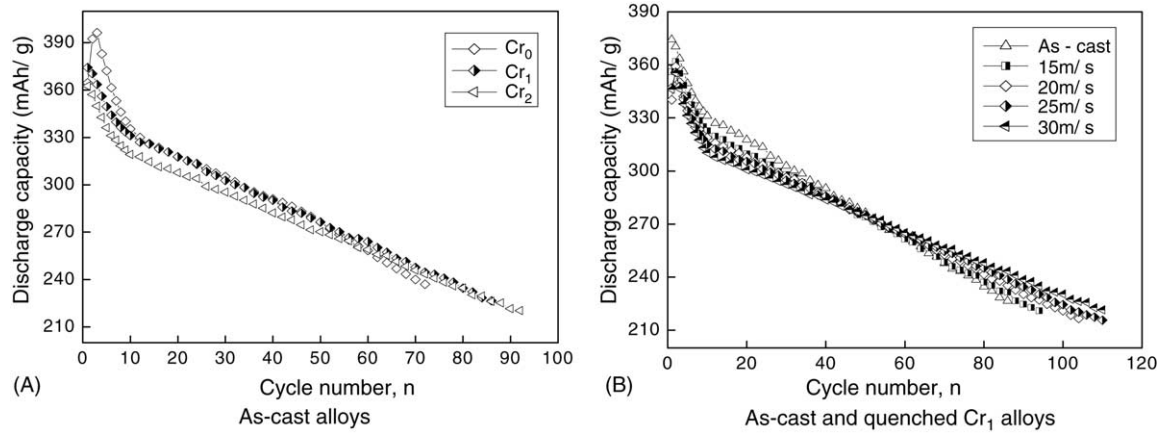

Fig. 3. The relationship between the cycle number and the discharge capacity: (a) as-cast alloys; (b) as-cast and -quenched Cr_1 alloys.

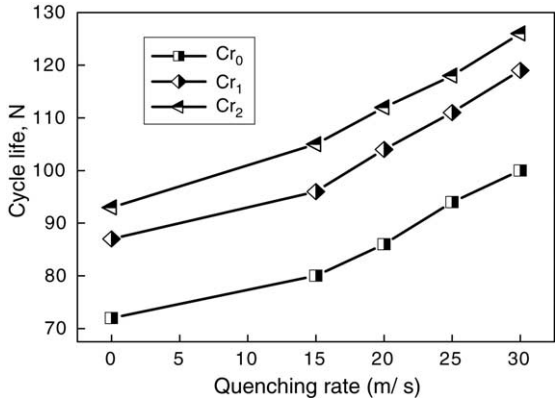

Fig. 4. The relationship between the quenching rate and the cycle life.

increase with the increase of Cr content. When the Cr content increases from 0 to 0.2, the cycle life of the as-cast alloy is enhanced from 72 cycles to 93 cycles. For the as-quenched alloys obtained with a quenching rate of 15 m s^{-1}, the cycle lives were enhanced from 80 to 105 cycles. The cycle lives of the alloys increase with the increase of the quenching rate. When the quenching rate increases from 0 to 30 m s^{-1}, the cycle lives of the Cr_0, Cr_1, Cr_2 alloys are enhanced from 72, 87, 93 to 100, 119, 126 cycles, respectively.

3.2. Microstructure

3.2.1. Phase composition and structure

The XRD patterns of the as-cast and -quenched alloys are shown in Fig. 5. It can be seen from Fig. 5(a) that no new phase is formed in alloys with Cr, but the main diffraction peaks of the $LaNi_5$ phase and $LaNi_3$ phase are nearly overlapping, and the amount of the $LaNi_2$ phase increase significantly. The effect of the rapid quenching on the amount of the $LaNi_2$ phase is unperceivable. The fact that the addition Cr increases the amount of the $LaNi_2$ phase shows the relative amount of the phases in the alloys change with the variety of the alloy component.

3.2.2. Microstructure and morphology

The morphologies of the as-cast and -quenched alloys were observed by SEM, and the results are shown in Fig. 6. According to the results obtained by energy spectrum analysis, the areas A, B are the $LaNi_5$ phase and (La, Mg)Ni_3 phase, respectively, and there is a specific amount of the $LaNi_2$ phase close to the (La, Mg)Ni_3 phase, but it is difficult to distinguish $LaNi_2$ phase and (La, Mg)Ni_3 phase by the observation of the microstructure and morphology. This is probably because the $LaNi_2$ phase adheres to the (La, Mg)Ni_3 phase grew in the process of the crystallization. The morphologies and the crystalline states of the as-quenched alloys were examined by TEM, and the results are shown in Fig. 7. It can be seen from Fig. 7 that the grains of the alloy are refined markedly with the increase of the quenching rate. And the phase structure of the alloy change from nanocrystalline phase to the amorphous phase when the quenching rate increases from 15 to 30 m s^{-1}. The results obtained by SAD (Fig. 7(b) and (d)) with different quenching rate show that the alloys present a multiphase, integral crystal structure when the quenching rate is 15 m s^{-1}, and a trend of the amorphous phase formation is very obvious in as-quenched alloy with the quenching rate of 30 m s^{-1}.

Generally, the activation performance of the electrode alloy is closely related to the phase structure, the surface characteristic, the grain size and the interstitial dimensions of the alloy. The fact that the as-cast and -quenched alloys have

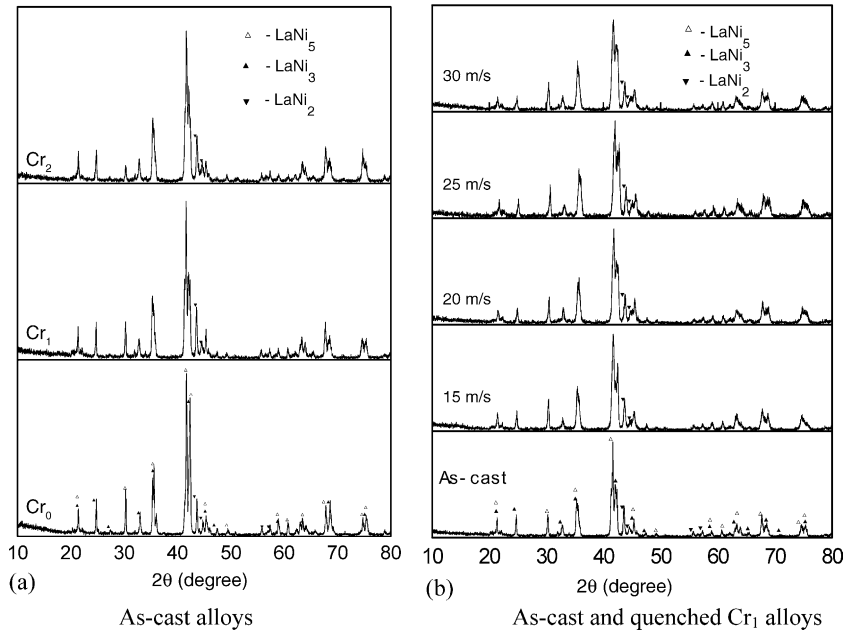

Fig. 5. The X-ray diffraction patterns of the as-cast and -quenched alloys: (a) as-cast alloys; (b) as-cast and -quenched Cr_1 alloys.

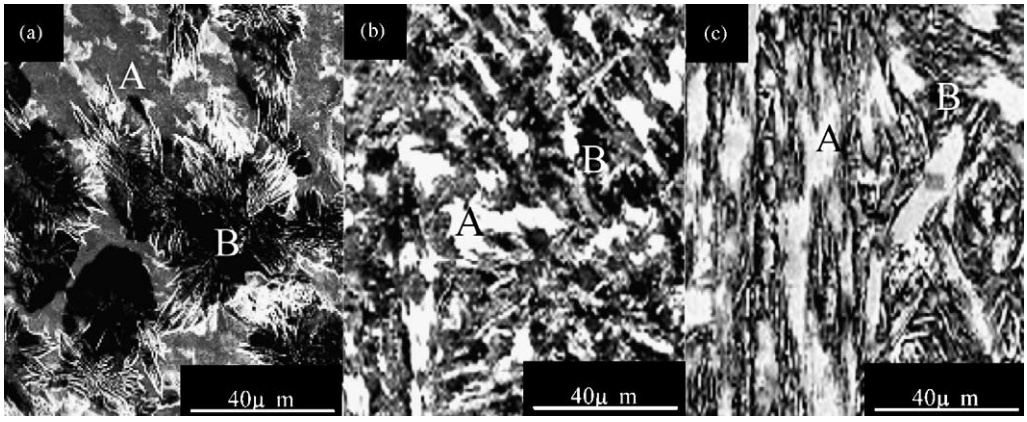

Fig. 6. The morphologies of the as- alloys taken by TEM: (a) Cr_0 alloy; (b) Cr_1 alloy; (c) Cr_2 alloy.

good activation performances is mainly ascribed to their multiphase structures because the phase boundary can decrease the lattice distortion and strain energy formed in the process of hydrogen absorption. Furthermore, the phase boundary provides good tunnels for diffusion of hydrogen atoms and the activation performance of the alloys is improved significantly. The main cause that the addition Cr improves the activation performance of the as-cast alloy is that Cr increases the amount of the $LaNi_2$ phase and phase boundary area.

The addition Cr decreasing the capacities of the as-cast alloys is attributed to the increase of the amount of the $LaNi_2$ phase. The capability of the hydrogen absorption of the $LaNi_2$ phase is much lower than that of the (La, Mg) Ni_3 phase and the $LaNi_5$ phase. So, the more the amount of the $LaNi_2$ phase, the smaller the capacity of the alloy. In addition, the capacity of the alloy decreases with the increase of the quenching rate, it being relative to rapid quenching changing the microstructure of the alloy. According to the analysis of the microstructure, the rapid quenching refines greatly the grain of the alloy, and the higher the quenching rate, the finer the grain of the alloy. An amorphous phase is formed at the specific quenching rate. The influence of the rapid quenching on the discharge capacity is complicated. Both the increase of the lattice constants and the decrease of the grain size as necessary results

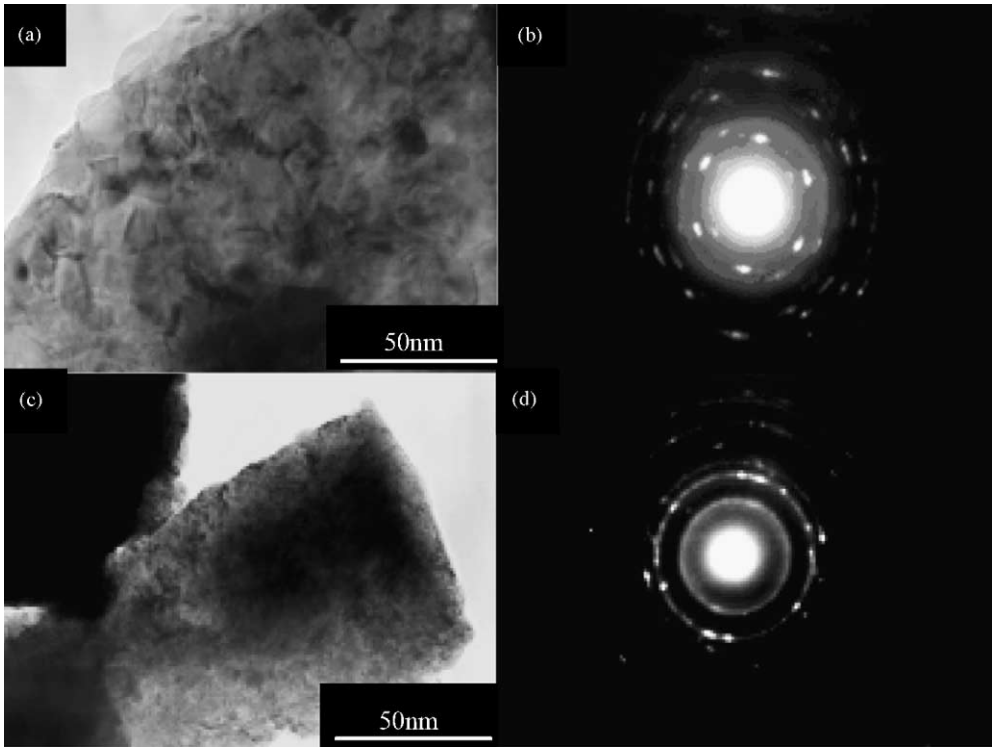

Fig. 7. The morphologies and SAD of the as-quenched Cr_1 alloys: (a) and (c) morphologies of as-quenched Cr_1 alloys (15, 30 m s^{-1}); (b) and (d) SAD of as-quenched Cr_1 alloys (15 and 30 m s^{-1}).

of the rapid quenching are favourable for the capacity on one hand, but the formation of an amorphous phase produced by rapid quenching is unfavourable on the other hand. Therefore, whether rapid quenching would increase or decrease the discharge capacity of the alloy depends on the relative predominance of the above-mentioned effects. We considered that the effect of the amorphous phase is much stronger. Li and Cheng [11] investigated the hydrogen absorbing capability of La–Ni alloy amorphous film, and the results showed the capacity of the amorphous film was half as large as that of the crystal alloy. Therefore, the greater the quenching rate, the more the amount of amorphous phase, the smaller the capacity of the alloy.

The cycle stability of electrode alloy is an overwhelming factor of the life of Ni-MH battery. The root cause of leading to battery lose efficacy is on negative electrode rather than on positive electrode. The failure of battery is characterized by the decay of the discharge capacity and the decrease of the discharge voltage. It can be derived from the literatures [12–15] that the fundamental reasons for the capacity decay of the electrode alloy are the pulverization and oxidation of the electrode alloy during the charge–discharge cycles. The lattice internal stress and cell volume expansion, which are inevitable when hydrogen atoms enter into the interstitials of the lattice, are the real driving force that leads to the pulverization of the alloy. In order to understand correctly the mechanism of the efficacy loss of the electrode alloy, the morphologies of the as-cast and -quenched alloy particles before and after electrochemical cycle as observed by SEM are shown in Fig. 8. It can be seen from Fig. 8 that the changes of the granule sizes of the as-cast and -quenched alloys before and after electrochemical cycle are insignificant. The result shows that the pulverization does not basically occur in process of the charge–discharge cycle. This indicates that the oxidation and corrosion of the alloy electrode surface in corrosive electrolyte are main reasons of leading to the efficacy loss of the alloy electrode. The formation of an oxidation and corrosion layer on the surface of the alloy electrode baffles the diffusion of hydrogen atoms, and decreases the dynamical property in the process of hydrogen absorption and desorption. Therefore, it can be concluded that the most important approach of enhancing the cycle life of the La–Mg–Ni system ($PuNi_3$-type) hydrogen storage electrode alloy is to improve the anti-corrosion and oxidation capabilities of the alloy in corrosive electrolyte. The function of addition Cr on the electrochemical stability of the as-cast alloy is relative to the formation of the $LaNi_2$ phase. The electrocatalytic activation of $LaNi_2$, $LaNi_3$ and $LaNi_5$ phases in alloy increases in the sequence $LaNi_2 < LaNi_3 < LaNi_5$. The lanthanum in the $LaNi_2$ phase is eroded by the alkaline electrolyte during the electrochemical cycle. Thus, the electrocatalytic activation of the $LaNi_2$ phase is significantly improved, and the capabilities of hydrogen absorption and desorption are enhanced [16,17]. The capacity decay of the alloy can partly be compensated by the power produced by the $LaNi_2$ phase. In addition, Cr can improve the anti-corrosion capability of the alloy. It was suggested that the effect of Si, Cr, and Al addition led to the formation of a passivating oxide layer on the alloy surface which would prevent further oxidation of the inner alloy [13,18,19]. The detailed mechanisms need to

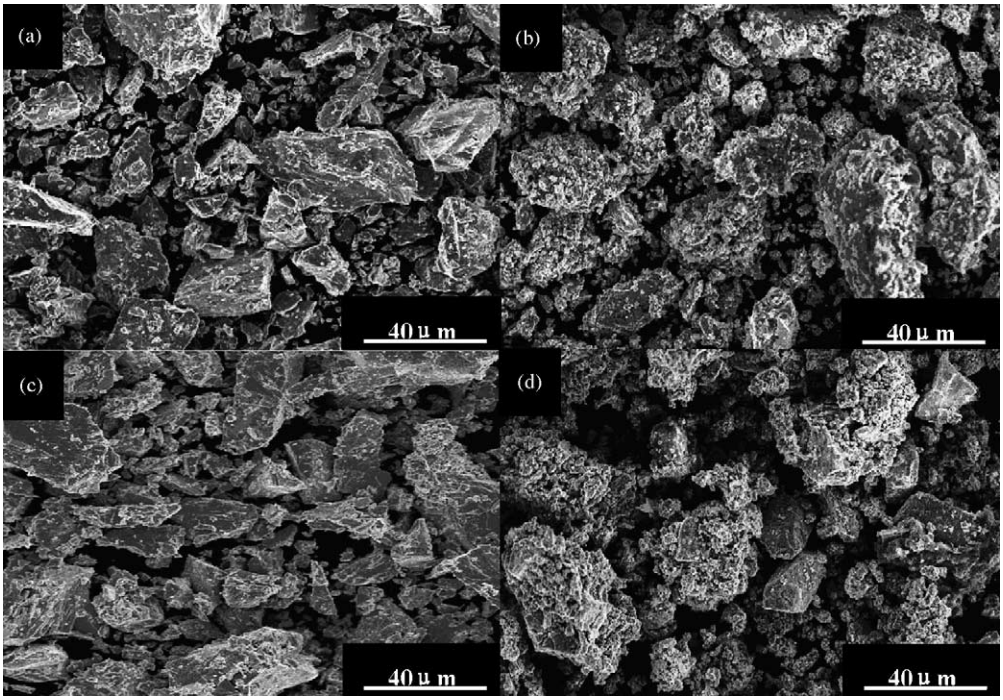

Fig. 8. The granular morphologies of as-cast and -quenched Cr_1 alloy before and after electrochemical cycle (SEM): (a) and (b) as-cast Cr_1 alloy before and after cycle; (c) and (d) as-quenched Cr_1 alloy before and after cycle (15 m s^{-1}).

be investigated further. The reason of the rapid quenching improving the cycle stability of the alloy is that a special structure obtained by the rapid quenching enhances the anti-corrosion and oxidation capabilities of the alloy in corrosive electrolyte. Especially, the effect of the formation of an amorphous phase on improving the anti-corrosion capability of the alloy in corrosive electrolyte is notable [20–22]. However, it is difficult for rapid quenching to obtain more amorphous phase in the La–Mg–Ni system ($PuNi_3$-type) alloy. Therefore, the function of the rapid quenching on the cycle life of the alloy is very limited.

4. Conclusions

1. The as-cast and -quenched $La_2Mg(Ni_{0.85}Co_{0.15})_9Cr_x$ ($x = 0$, 0.1, 0.2) electrode alloys have a multi-phase structure, including the (La,Mg)Ni_3 phase, the $LaNi_5$ phase and a small amount of the $LaNi_2$ phase. The relative amount of each phase in the alloy depends on the composition of the alloy. The addition Cr is favourable for the formation of the $LaNi_2$ phase in the as-cast alloy.
2. The addition Cr decreasing the capacities of the as-cast alloys is attribute to the increase of the $LaNi_2$ phase. The capacities of the alloys decrease with the increase of the quenching rate. It is mainly ascribed to the formation of an amorphous phase in the alloy after rapid quenching.
3. The addition Cr improves the cycle life of the as-cast alloy because Cr increases the $LaNi_2$ phase in the as-cast alloy and improves the anti-corrosion capability of the alloy in corrosive electrolyte. The cycle lives of the alloys increase with the increase of the quenching rate. The main reason is the formation of a specific amount of amorphous phase in the as-quenched alloy.
4. The root cause of leading to La–Mg–Ni system ($PuNi_3$-type) alloy lose efficacy is oxidation and corrosion of the electrode surface in process of electrochemical cycle. The most effective approach of enhancing the cycle life of the La–Mg–Ni system ($PuNi_3$-type) hydrogen storage electrode alloy is to improve the anti-corrosion and oxidation capabilities of the alloy in corrosive electrolyte.

Acknowledgements

This work is supported by National Natural Science Foundations of China (50131040).

References

[1] T. Sakai, H. Miyamura, N. Kuriyama, A. Kato, K. Oguro, H. Ishikawa, J. Electrochem. Soc. 137 (1990) 795.
[2] J.J.G. Willems, K.H.J. Buschow, J. Less-Comm. Met. 129 (1987) 13.
[3] S.R. Ovshinsky, M.A. Fetcenko, J. Ross, Science 260 (1993) 176.
[4] M. Tsukahara, T. Kamiya, K. Takahashi, A. Kawabata, S. Sakurai, J. Shi, H.T. Takeshita, N. Kuriyama, T. Sakai, J. Electrochem. Soc. 147 (2000) 2941.
[5] D. Sun, H. Enoki, F. Gingl, E. Akiba, J. Alloys Compd. 285 (1999) 279.
[6] T. Kohno, H. Yoshida, F. Kawashima, T. Inaba, I. Sakai, M. Yamamoto, M. Kanda, J. Alloys Compd. 311 (2000) 5.
[7] W.-K. Hu, J. Alloys Compd. 297 (2000) 206.
[8] H. Oesterreicher, H. Bittner, J. Less-Comm. Met. 73 (1980) 339.
[9] K. Kadir, I. Uehara, T. Sakai, J. Alloys Compd. 257 (1997) 115.
[10] H. Pan, Y. Liu, M. Gao, Y. Zhu, Y. Lei, Q. Wang, J. Alloys Compd. 351 (2003) 228.
[11] Y. Li, Y.T. Cheng, J. Alloys Compd. 223 (1995) 6.
[12] D. Chartouni, F. Meli, A. Züttel, K. Gross, L. Schlapbach, J. Alloys Compd. 241 (1996) 160.
[13] T. Sakai, K. Oguro, H. Miyamura, N. Kurayama, A. Kato, H. Ishikawa, J. Less-Comm. Met. 161 (1990) 193.
[14] A.H. Boonstra, T.M.N. Bernards, J. Less-Comm. Met. 161 (1990) 355.
[15] A.H. Boonstra, T.M.N. Bernards, J. Less-Comm. Met. 161 (1990) 245.
[16] Y. Bo, C. Lian, W. Mingfen, T. Min, L. Ribin, T. Yanwen, Z. Yuchun, Acta Metall. Sinica 35 (10) (1999) 1069.
[17] M. Ikoma, K. Komori, S. Kaida, C. Iwakura, J. Alloys Compd. 284 (1999) 92.
[18] T. Sakai, T. Hazama, H. Miyamura, N. Kuriyama, A. Kato, H. Ishikawa, J. Less-Comm. Met. 172–174 (1991) 1175.
[19] J.M. Cocciantelli, P. Bernard, S. Fernandez, J. Atkin, J. Alloys Compd. 253/254 (1997) 642.
[20] C.-J. Li, F.-R. Wang, W.-H. Cheng, W. Li, W.-T. Zhao, J. Alloys Compd. 315 (2001) 218.
[21] Y.-H. Zhang, M.-Y. Chen, X.-L. Wang, G.-Q. Wang, Y.-F. Lin, Y. Qi, J. Power Sources 125 (2004) 273.
[22] Y.-H. Zhang, M.-Y. Chen, X.-L. Wang, G.-Q. Wang, X.-P. Dong, Y. Qi, Electrochem. Acta 49 (2004) 1161.